

New Study on Soil Liquefaction Susceptibility Categories

Chin-Hsun Yeh¹, Gee-Yu Liu¹ and Lee-Hui Huang¹

Abstract

Soil liquefaction is one of the major geo-hazards caused by large earthquakes. Some of buildings, bridges and buried pipelines in the severe liquefied regions may damage or loss of functions. In order to identify the probable liquefied regions and to assess the amount of settlement and the degree of influence on various kinds of civil infra-structures, it is necessary to have a feasible and effective method to assess the soil liquefaction probability and the associated settlement in wide area due to scenario earthquakes. A methodology of earthquake scenario simulation and risk assessment, that is, Taiwan Earthquake Loss Estimation System (TELES) has been developed by the National Center for Research on Earthquake Engineering (NCEE) in Taiwan. Integrating the concept of soil liquefaction susceptibility categories in HAZUS and the engineering borehole data from the Central Geological Survey Bureau of Taiwan, a set of empirical formulas for each soil liquefaction susceptibility category was proposed in TELES to assess soil liquefaction potential index and the associated settlement. The peak ground acceleration (A), earthquake magnitude (M) and ground-water depth (D) were taken into account in deriving the empirical formulas. Besides reviewing the existing analysis model and empirical formula, this paper intends to reinvestigate the classification scheme of soil liquefaction susceptibility categories, to propose a new functional form for empirical formula, and to modify the interpretation of liquefaction potential index. A soil liquefaction susceptibility category map of Taiwan will also be updated by using additional borehole and geologic data. The scenario simulation results and the probable applications will be discussed.

Keywords: soil liquefaction susceptibility category, liquefaction potential index, settlement

Review of Existing Soil Liquefaction Assessment Model

When saturated loose soil is subjected to cyclic loadings, and if the vibration is large enough and lasts for a long time, the soil particles will tend to rearrange their relative positions, the volume tends to shrink due to gravity, the pore-water pressure increases rapidly, and soil liquefaction phenomenon will occur. Generally speaking, the ground shaking intensity, duration and ground-water depth are three major factors that will influence soil liquefaction potential and the associated severity of settlement or lateral spreading. To simplify liquefaction assessment model, the peak ground acceleration and the earthquake magnitude are commonly used to indicate the excitation intensity and the duration of excitation, respectively.

¹ National Center for Research on Earthquake Engineering, National Applied Research Laboratories, 200, Sec. 3, Xinhai Rd., Daan, Taipei, Taiwan

Liquefaction Susceptibility Categories

According to the earthquake loss estimation methodology of HAZUS (RMS, 1997), the soil liquefaction susceptibility at a site was classified into six categories, that is, "very high", "high", "moderate", "low", "very low" and "none" susceptibility. The empirical formulas for each category to estimate the liquefaction probability and the induced permanent ground deformation were also provided in the technical manual. However, the classification scheme proposed in HAZUS for soil liquefaction susceptibility was not based on operational definitions or quantitative descriptions. To overcome the shortcomings, a modified classification scheme for soil liquefaction susceptibility was proposed by Yeh, et al (2002) and had been used in TELES. The modified classification scheme was based on layer properties, such as SPTN and fine content, of engineering borehole data.

In Yeh, et al. (2002), a soil liquefaction potential index (P_L) proposed by Iwasaki, et al. (1982) was used to estimate the liquefaction potential and severity at the site subjected to any combination of peak ground acceleration, earthquake magnitude and ground-water depth. Comparing many liquefied and non-liquefied cases after strong earthquakes, Iwasaki, et al. (1982) found that in case $P_L \geq 15$, the liquefaction probability is high and the sites may be severely liquefied; on the other hand, if $P_L \leq 5$, the liquefaction probability is low and the sites may not be liquefied at all. In the classification scheme, according to Yeh, et al. (2002), the earthquake magnitude and the ground-water depth are assumed to be constant (7.5 and 1.5 meters, respectively) but the level of ground shaking in terms of peak ground acceleration (PGA) was gradually increased to determine the threshold when $P_L \geq 15$. The boreholes with $P_L \geq 15$, when PGA were 0.15g, 0.2g, 0.25g, 0.35g and 0.45g, belong to "very high", "high", "moderate", "low" and "very low" susceptibility categories, respectively. All the other boreholes with $P_L < 15$, when PGA is 0.45g, were classified as "none" sensitive to soil liquefaction.

Empirical Formulas for Estimating Liquefaction Potential

From figures of P_L versus PGA for different susceptibility categories and under various earthquake magnitude and ground-water depth, it is noted that the relationships between P_L and PGA are almost linear within the range $5 \leq P_L \leq 20$. Thus, for simplicity and suggested in HAZUS, the empirical formulas of liquefaction potential index for different susceptibility category i were expressed as follows in Yeh, et al (2002) study:

$$P_{L,i} = \alpha_i \cdot f(M) \cdot g(D) \cdot A + \beta_i \quad (1)$$

Where A was the peak ground acceleration at the site; subscript i indicates susceptibility category; α_i and β_i were constants and listed in Table 1. The modification functions due to earthquake magnitude (M) and ground-water depth (D) were not sensitive among different liquefaction susceptibility categories and can be expressed as follows:

$$f(M) = 0.0353M^2 - 0.1855M + 0.4069 \quad (2)$$

$$g(D) = 0.0002D^4 - 0.0051D^3 + 0.0535D^2 - 0.2758D + 1.3105 \quad (3)$$

Table 1 Values of α_i and β_i in Eq. (1).

Category	α_i	β_i
Very High	227.52	-13.63
High	188.30	-18.45
Moderate	157.35	-20.51
Low	103.02	-14.95
Very Low	66.95	-10.64

Empirical Formulas for Estimating Settlement

Ishihara (1993) proposed a method to estimate settlement due to soil liquefaction. Ge (1997) made some assumptions and used a nonlinear regression method to analyze the Ishihara's data and proposed analytic formulas to estimate liquefaction settlement. From figures showing relationship of settlement versus PGA for different combinations of earthquake magnitude and ground-water depth, it can be seen that the amount of settlement approaches a limiting value when PGA becomes larger; and the limiting value depends only on the susceptibility category. Since the relationship of settlement versus PGA was similar to a log-normal distribution function, only two parameters, that is, median and log-standard deviation were required to describe the relationship.

In Yeh, et al (2002) study, the relationship of liquefaction settlement (S) versus peak ground acceleration (A) were expressed as

$$S = \bar{S}_i \cdot \Phi \left[\frac{\ln(A / m_i)}{\sigma_i} \right] \quad (4)$$

where \bar{S}_i is the limiting value for susceptibility category i ; $\Phi(\cdot)$ is the standard normal distribution function; and m_i and σ_i are the median and the log-standard deviation of the log-normal distribution function, respectively. It is noted that m_i and σ_i are functions of earthquake magnitude and ground-water depth; but the modification functions due to earthquake magnitude ($\bar{f}(M)$) and ground-water depth ($\bar{g}(D)$ and $\bar{h}(D)$) were not sensitive to liquefaction susceptibility category. Thus, m_i and σ_i were expressed as follows:

$$m_i = \mu_i \cdot \bar{f}(M) \cdot \bar{g}(D) \quad (5)$$

$$\sigma_i = \lambda_i \cdot \bar{h}(D) \quad (6)$$

$$\bar{f}(M) = 0.1231M^2 - 2.2052M + 10.5954 \quad (7)$$

$$\bar{g}(D) = -0.007188D^2 + 0.145195D + 0.7919 \quad (8)$$

$$\bar{h}(D) = 0.003208D^2 - 0.042231D + 1.0611 \quad (9)$$

where μ_i and λ_i were constants and listed in Table 2.

Table 2 Values of \bar{S}_i , μ_i and λ_i in Eq. (4).

Category	\bar{S}_i (cm)	μ_i (g)	λ_i
Very High	47.43	0.0872	0.4522
High	50.22	0.1292	0.3657
Moderate	46.21	0.1613	0.3433
Low	35.89	0.1875	0.3430
Very Low	25.66	0.2104	0.3764

Updated Soil Liquefaction Assessment Model

Although the previous observations and empirical formulas for soil liquefaction potential and settlement have been proved to be useful, it needs improvement. For example, use of a linear form in Eq. (1) could not distinguish effectively the relative potential at two different sites where P_L were both greater than 20. In addition, as shown in Figure 1, the liquefaction potential index should have an upper limit and is seldom larger than 70. However, the predicated P_L does not saturate when PGA is large by using Eq. (1).

Classification Scheme of Soil Liquefaction Susceptibility

To increase resolution of soil liquefaction susceptibility for different soil conditions using borehole data, the soil liquefaction susceptibility was classified into ten categories. They are designated from category 9 to category 0. The category 9 corresponds to the most sensitive soil site, while category 0 correspond to none sensitive soil or rock sites. Similar to the approach in Yeh, et al (2002), under constant earthquake magnitude ($M_w = 7.5$) and ground-water depth (1.5 m), the PGA threshold of $P_L \geq 15$ for various kinds of liquefaction susceptibility categories fall within the ranges divided by 0.15g, 0.2g, 0.25g, 0.3g, 0.35g, 0.4g, 0.45g, 0.5g, 0.6g, respectively. For example, $P_L \geq 15$ when PGA is less than 0.15g at the most sensitive sites (category 9); $P_L \geq 15$ when PGA is greater than 0.15g but less than 0.2g at the second sensitive sites (category 8), and so on.

Comparing with the existing classification scheme for soil susceptibility categories, the categories 9, 8 and 7 correspond to categories "very high", "high" and "moderate" susceptibility, respectively. The original "low", "very low" and "none" susceptibility categories are partitioned into seven sub-categories to increase recognition of different soil conditions.

Empirical Formula for Soil Liquefaction Potential Index

Figure 1 shows a plot of soil liquefaction potential index (P_L) versus peak ground acceleration (PGA) for category 9 with different ground-water depth and subjected to the same earthquake magnitude (7.5). As shown in the figure, the P_L approaches to a limiting value when PGA becomes larger and larger. Furthermore, through nonlinear regression, it

can be shown that the limiting values of P_L depend on the earthquake magnitude and the ground-water depth, as shown in Figure 2. To assess P_L more accurately, a log-normal distribution function, instead of a linear function in Eq. (1), was used to describe the nonlinear relationship between P_L and PGA subjected to different combinations of earthquake magnitude and ground-water depth. In other words, the estimated P_L can be expressed as:

$$P_{L,i} = u_{i,PL} \cdot \Phi \left[\frac{\ln(A/m_{i,PL})}{\beta_{i,PL}} \right] \quad (10)$$

where subscript i indicates susceptibility category; $u_{i,PL}$, $m_{i,PL}$ and $\beta_{i,PL}$ are upper-limit of P_L , median value of PGA and log-standard deviation of the log-normal distribution function, respectively. The $u_{i,PL}$, $m_{i,PL}$ and $\beta_{i,PL}$ are functions of earthquake magnitude and ground-water depth, and can be expressed as follows:

$$u_{i,PL} = K_{u,i} \cdot (-0.01729M^2 + 0.3072M - 0.331) \cdot (0.000916D^2 - 0.01578D + 1) \quad (11)$$

$$m_{i,PL} = K_{m,i} \cdot (-0.03907M^3 + 0.9699M^2 - 8.236M + 24.7) \cdot (0.001021D^3 - 0.02482D^2 + 0.234D + 1) \quad (12)$$

$$\beta_{i,PL} = K_{\beta,i} \cdot (-0.00739M^3 + 0.1404M^2 - 0.726M + 1.665) \cdot (-0.0000871D^3 + 0.004257D^2 - 0.05307D + 1) \quad (13)$$

where $K_{u,i}$, $K_{m,i}$ and $K_{\beta,i}$ are constants and listed in Table 3. As shown above, the variations of $u_{i,PL}$, $m_{i,PL}$ and $\beta_{i,PL}$ with respect to earthquake magnitude and ground-water depth for different susceptibility categories are almost the same and can be approximated by the same functions. The anchor-point in evaluation of $K_{u,i}$, $K_{m,i}$ and $K_{\beta,i}$ is earthquake magnitude 7.5 and ground-water depth 0 meter.

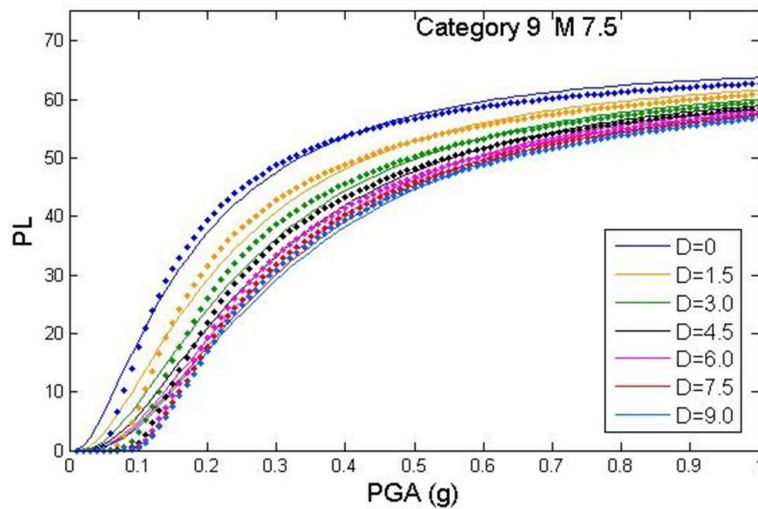


Fig. 1 Plot of P_L versus PGA for category 9 with different ground-water depth and subjected to earthquakes with magnitude 7.5.

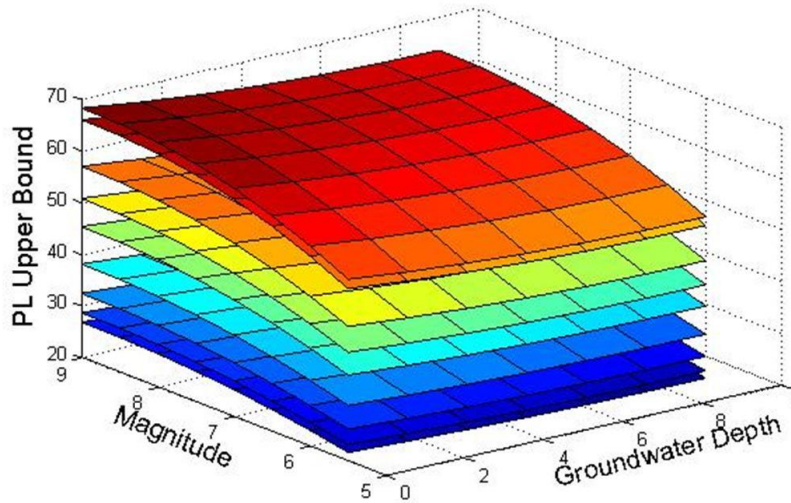


Fig. 2 Upper bounds for plot of P_L versus PGA under different combinations of earthquake magnitude and ground-water depth.

Table 3 Values of $K_{u,i}$, $K_{m,i}$ and $K_{\beta,i}$ in Eq. (11), (12) and (13), respectively.

Susceptibility Category	$K_{u,i}$	$K_{m,i}$	$K_{\beta,i}$
Category 9	65.86	0.1712	0.9540
Category 8	63.69	0.2280	0.8275
Category 7	54.97	0.2630	0.7646
Category 6	48.98	0.2949	0.7234
Category 5	43.72	0.3213	0.6963
Category 4	36.71	0.3354	0.6840
Category 3	31.22	0.3354	0.7013
Category 2	27.60	0.3394	0.7095
Category 1	25.83	0.3557	0.6871

Empirical Formula for Settlement due to Soil Liquefaction

Applying a similar procedure on the analysis of settlement due to soil liquefaction, Figure 3 shows a plot of settlement versus peak ground acceleration (PGA) for category 9 with different ground-water depth and subjected to the same earthquake magnitude (7.5). As shown in the figure, the amount of settlement due to liquefaction approaches to a limiting value when PGA becomes larger and larger. Secondly, the limiting value does not change with different ground-water depth. If the nonlinear relationship of settlement and PGA was described by a log-normal distribution function, which was obtained by nonlinear regression technology, can be expressed as follows:

$$S_i = u_{i,S} \cdot \Phi \left[\frac{\ln(A / m_{i,S})}{\beta_{i,S}} \right] \quad (14)$$

where subscript i indicates susceptibility category; $u_{i,S}$, $m_{i,S}$ and $\beta_{i,S}$ are upper-limit of settlement, median value of PGA and log-standard deviation of the log-normal distribution function, respectively. As can be seen from the results of nonlinear regression, the upper-limit and the log-standard deviation of the log-normal distribution function, that is, $u_{i,S}$ and $\beta_{i,S}$ almost keep constant for the same soil liquefaction susceptibility category. However, the median value ($m_{i,S}$) of log-normal distribution function does vary with respect to earthquake magnitude and ground-water depth. In summary, the $u_{i,S}$, $m_{i,S}$ and $\beta_{i,S}$ can be expressed as follows:

$$u_{i,S} = S_{u,i} \quad (15)$$

$$\beta_{i,S} = S_{\beta,i} \quad (16)$$

$$m_{i,S} = S_{m,i} \cdot (-0.05693M^3 + 1.4192M^2 - 12.0101M + 35.263) \cdot (-0.000483 D^3 - 0.01458D^2 + 0.1897D + 1) \quad (17)$$

where $S_{u,i}$, $S_{m,i}$ and $S_{\beta,i}$ are constants and listed in Table 4. As is implied in Eq. (17), the variation of $m_{i,S}$ with respect to earthquake magnitude (M) and ground-water depth (D) is almost the same for different susceptibility categories and can be approximated by the same functions. The anchor-point in evaluation of $S_{m,i}$ is earthquake magnitude 7.5 and ground-water depth 0 meter.

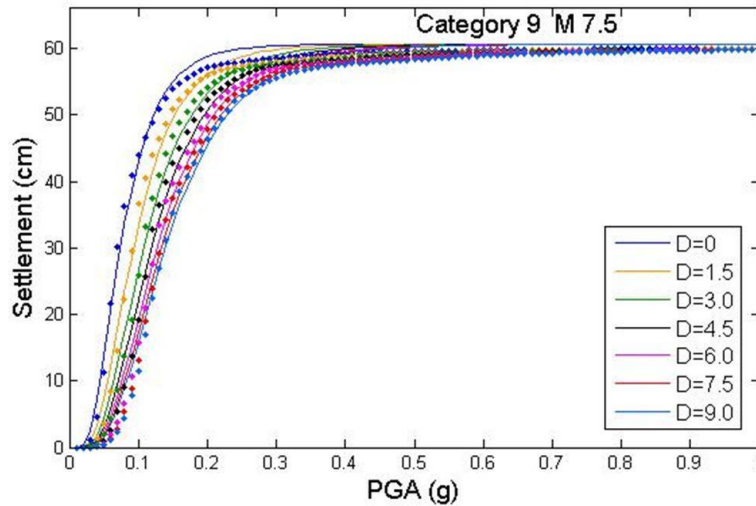


Fig. 3 Plot of settlement versus PGA for category 9 with different ground-water depth and subjected to earthquakes with magnitude 7.5.

Table 4 Values of $S_{u,i}$, $S_{m,i}$ and $S_{\beta,i}$ in Eq. (15), (16) and (17), respectively.

Susceptibility Category	$S_{u,i}$	$S_{m,i}$	$S_{\beta,i}$
Category 9	60.64	0.0746	0.5276
Category 8	52.09	0.1052	0.5318
Category 7	42.36	0.1276	0.5572
Category 6	34.99	0.1452	0.6065
Category 5	30.69	0.1643	0.6583
Category 4	25.69	0.1697	0.6687
Category 3	20.30	0.1683	0.6951
Category 2	18.25	0.1651	0.6908
Category 1	15.78	0.1742	0.7169

Discussion

A liquefaction potential index proposed by Iwasaki, et al. (1982) has been commonly used in engineering society to indicate the liquefaction potential and severity at the sites during strong earthquakes. Using the updated classification scheme for soil liquefaction susceptibility, it is possible to distinguish liquefaction potential in the original "low", "very low" and "none" susceptibility sites. Use of log-normal distribution function in the empirical formulas may improve accuracy in estimating liquefaction potential index; it also provides a natural way to assign liquefaction probability at the sites in scenario earthquakes. Liquefaction susceptibility category map of Taiwan will be updated later and applications to probabilistic seismic hazard analysis will be studied, too.

References

- Risk Management Solutions, 1997. "Earthquake Loss Estimation Method—HAZUS97 Technical Manual", National Institute of Building Sciences, Washington, D.C.
- Yeh, C. H., Hsieh, M. Y., and Loh, C. H., 2002. "Classification and Parametric Study on Soil Liquefaction Potential", *Proceedings of Second Japan-Taiwan Workshop on Lifeline Performance and Disaster Mitigation*, Kobe University, Japan.
- Iwasaki, T., Arakawa, T., and Tokida, K., 1982. "Simplified Procedures for Assessing Soil Liquefaction during Earthquake", *Proceedings of the Conference on Soil Dynamics & Earthquake Engineering*, Vol. II, 925-939.
- Ishihara, k., 1993. "Liquefaction and Flow Failure during Earthquake", *Geotechnique* 43 (3), 315-415.
- Ge, W. Y., 1997. "Liquefaction Settlement and Potential Analysis of Sediment in Yung-an, Kaohsiung Area", Ph.D. dissertation, Civil Eng. Dept., National Cheng-Kung University.